Proceedings of ALGORITMY 2005
pp. 123–131

INFLUENCE OF MESH GEOMETRY TO NUMERICAL DIFFUSION IN UPWIND SCHEME FOR POROUS MEDIA SOLUTE TRANSPORT*

MILAN HOKR† AND JIŘÍ MARYŠKA†

Abstract. We present results of experiments showing the character of numerical diffusion in solute transport model with explicit upwind finite volume scheme, under two influences: perturbation of mesh (small random change of node positions) and angle between fluid velocity and characteristic directions of the mesh. We observe situations, where the numerical diffusion in 2D can be identified with longitudinal and transversal hydrodynamic dispersion coefficients, used for the porous media transport description. In these cases, the numerical error corresponds to parameter uncertainty, which can be a reason why a software with basic numerical methods can produce results satisfactory in the application.

Key words. mesh perturbation, hydrodynamic dispersion, groundwater models, advection-diffusion

AMS subject classifications. 65P05, 76R99, 76S05

1. Introduction. Solution of advection-diffusion problems is one of the challenges for numerical mathematics. Although many sophisticated methods exist, we cannot in general avoid one of the characteristic difficulties – artificial oscillations or numerical diffusion [5], namely for the advection-dominated problems.

Here we consider the context of porous media solute transport, governed by the advection-diffusion/dispersion equation for unknown concentration $c(\vec{x}, t)$, function of space and time (see e.g. [1]):

$$\frac{\partial c}{\partial t} + \nabla \cdot (c\vec{v}) - \nabla \cdot (\mathbb{D}\nabla c) = \frac{1}{n}(c^* q_s^+ + c q_s^-)\,, \tag{1.1}$$

where $\vec{v}$ is the fluid velocity, $\mathbb{D}(\vec{v})$ is the hydrodynamic dispersion tensor, n is the porosity, q_s is fluid source/sink intensity, and c^* is the given concentration in the injection wells (sources). The hydrodynamic dispersion includes the molecular diffusion and mixing of variably concentrated solution in pores. In contrast with pure molecular diffusion, the hydrodynamic dispersion is anisotropic in principle.

In the porous media problems, the identification of dispersion coefficients is usually difficult and often the achieved accuracy is only the order of magnitude [8]. Typically, the problem is advection dominated, which is expressed in terms of Péclet number:

$$\mathrm{Pe} = \frac{|\vec{v}|d}{|\mathbb{D}|} \gg 1\,, \tag{1.2}$$

where d is a characteristic length of the solved problem. Thus there are less requirements of accuracy of numerical processing of hydrodynamic dispersion.

The classical solute transport codes used by hydrogeologists mostly use the basic numerical methods for calculating the advection and hydrodynamic dispersion process

*This work was supported with the subvention from Ministry of Education of the Czech Republic, project code 242200001.

†Department of Modelling of Processes, Technical University of Liberec, Czech Republic (milan.hokr@vslib.cz).

(e.g. the US Geological Survey models MF2K-GWT, i.e. the MODFLOW with simple particle tracking method on finite-difference mesh, or SUTRA using the finite elements with an optional upwinding). The approaches how to manage with the numerical diffusion mentioned in the user manuals are typically two: to be careful to have sufficiently fine mesh and/or to use the diffusion-dispersion coefficient reduced by the expected numerical diffusion [8]. On the other hand, no tools how to recognize the amount of numerical diffusion in complicated geometry are offered.

Since the origin of the numerical diffusion is in discretisation of the advective term, it appears to be useful to observe the behaviour of numerical methods for pure advection in the context of advection-dispersion problems. For one-dimensional uniform problems, the expression of the numerical diffusion by means of diffusion coefficient in the "equivalent" advection-diffusion equation is well known (the 2^{nd} order error in the first order approximation) [2, 6].

On the other hand, the straightforward theoretical expression is possible only locally for one node or element in more dimensional non-uniform meshes. As the first step to study the global description of numerical diffusion in more dimensions, we propose several numerical experiments to verify a possibility to represent the numerical diffusion by means of equivalent physical parameters – the porous media hydrodynamic dispersion (the anisotropic process with two diffusion/dispersion coefficients in two directions, longitudinal and transversal with respect to the water velocity [8]). It is not a-priori clear if such a representation is possible, but it appears to be very illustrative in the context of porous media transport – we express the numerical error in terms of physical parameter uncertainty.

The study to find a relation between numerical diffusion and hydrodynamic dispersion is also motivated by a technique [7] how to employ the numerical diffusion as a part of the advection-dispersion problem solution in a specific 2D case: with the streamline-oriented mesh, the longitudinal dispersion is represented (replaced) by numerical diffusion of the scheme for advection and only the transversal dispersion is calculated explicitly (i.e. as a "real physical" dispersion). In other words – the advection problem is solved in the stream direction and the diffusion problem in the transversal direction.

In the cases of possible representation of numerical diffusion with hydrodynamic dispersion coefficients, the numerical models for solute transport get more efficiency and reliability: we can use either the calculation of pure advection or we know what change of physical parameters corresponds to the numerical error; i.e. also the basic numerical method can produce physically realistic results of porous media transport satisfactory for hydrogeologists.

2. Numerical method.

2.1. Finite-volume explicit upwind scheme. We consider the time-explicit scheme based on the finite-volume (FV) space discretisation with the mass fluxes calculated with upwind approximation [8, 2]. Defining the cell-centred representation [2] of unknown concentration (cell k, time $n\Delta t$)

$$C_k^n \approx \frac{1}{V_k} \int\limits_{V_k} c \,\mathrm{d}V \tag{2.1}$$

and the upwind flux approximation

$$\text{flux}[j-k] \approx C_k U_{kj} \text{ if } U_{kj} > 0 \text{ (from } V_k \text{ to } V_j)\,, \tag{2.2}$$

$$\text{flux}[j-k] \approx C_j U_{kj} \text{ if } U_{kj} < 0 \text{ (from } V_j \text{ to } V_k)\,, \tag{2.3}$$

we derive the FV scheme of the advection

$$C_k^{n+\frac{1}{2}} = C_k^n + \frac{\Delta t}{V_k} \cdot \big[- \sum_{j \in N_k} (U_{kj}^+ C_k^n + U_{kj}^- C_j^n) + C_k^n Q_k^- + \tilde{C}_k^n Q_k^+ \big] , \tag{2.4}$$

where Δt is the time step duration, Q_k is the source/sink intensity of fluid, $\tilde{C}_k^n$ is the injected concentration (given), V_k is the volume of the cell, N_k is the index set of neighbour cells. Next, U_{kj} are the fluxes from k-th cell to j-th cell, and the superscripts $+$ and $-$ behave as a "switch" between a positive or negative number ($a^+ = a$ for $a \geq 0$ and $a^+ = 0$ for $a < 0$ etc.).

2.1.1. Remark on implementation and interface. Even if we solve 2D problems in this paper, we work with the more general model based on the presented numerical method. The model is implemented as a 3D application for real-world underground contamination problems, with interface for general input data (unstructured 2D topology, cell-wise prescription of initial and boundary conditions). In this form, it was successfully applied for particular underground transport problems and also used as a base of model of non-equilibrium transport in dual-porosity media [3].

The model is connected to fluid flow model, providing the fluxes U_{kj} through cell sides (i.e. approximation of velocity field). In the mentioned application system as well as in our experiments the model based on mixed-hybrid finite element method is used [4]. For the experiments here (with a-priori given velocity field), the use of the flow model is just for convenience in processing of input data; the boundary conditions instead of the velocities/fluxes are entered.

2.2. Expression of numerical diffusion in 1D. With linear ordering of cells (1D problem), the FV scheme (2.4) corresponds to a finite difference scheme

$$C_k^{n+1} = C_k^n - v \frac{\Delta t}{\Delta x} (C_k^n - C_{k-1}^n) . \tag{2.5}$$

Through analysis of the second-order approximation error, the numerical diffusion (i.e. the coefficient at the second derivative) can be identified (see e.g. [2, 6])

$$D_{\text{num}} = \frac{1}{2} v \Delta x (1 - \text{Cr}) , \qquad \text{Cr} = \frac{v \Delta t}{\Delta x} , \tag{2.6}$$

where Δx is the mesh size and Cr is the Courant number, representing the stability condition $0 < \text{Cr} \leq 1$, which is a restriction for time step (to be sufficiently small).

In terms of our FV model, the Courant number can be expressed as the "non-overflow" condition for both outflow and inflow at each cell

$$\text{Cr} = \frac{\Delta t}{V_k} \big(Q_k^+ + \sum_{j \in N_k} U_{kj}^+ \big) = \frac{\Delta t}{V_k} \big(- Q_k^- + \sum_{j \in N_k} (-U_{kj}^-) \big) . \tag{2.7}$$

Understanding the mesh size Δx in the expression (2.6) as the distance of cell centres in the FV model, we can obtain the formula expressing the numerical diffusion in the 1D problems (or in any problem with appropriate "symmetry", i.e. orientation of mesh and velocity) solved by the FV scheme (2.4).

There is an open question concerning the behaviour of the model for general geometry of the problem (mesh structure, velocity orientation, etc.) in the sense of numerical diffusion in various direction (e.g. a possible representation by "longitudinal" and "transversal" coefficient, if adopting the terms of porous media hydrodynamic dispersion).

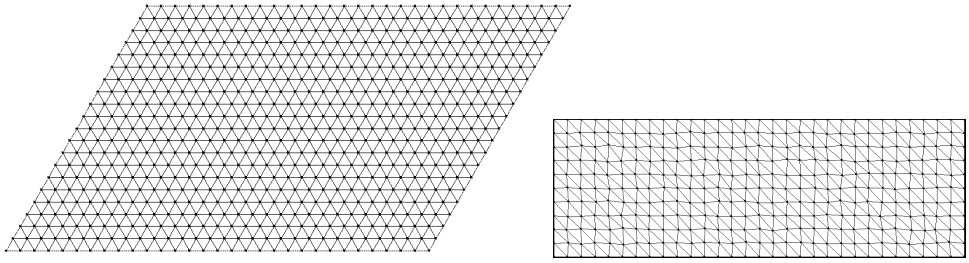

FIG. 3.1. *Meshes used for the experiments: rhomboidal domain with equilateral triangles, rectangular domain with squares/right triangles after random perturbation with variance* 0.5m.

2.3. Verification of estimates in 1D. Before solving and analysing more complex 2D problems, we tested first of all the expression of numerical diffusion in 1D. In other words, the validity of argumentation in the previous subsection generalising the finite-difference formula (2.6) to our FV scheme (replacing the meaning of Δx) is checked.

The results well correspond to expected 1D gaussian profile of diffusion/dispersion for Dirac initial condition. We note that the calculation is in fact numerically equivalent to the 1D finite-difference case (even if 3D basis of the model). The experiment also confirms the appropriateness of representing the Dirac initial condition in the numerical model (with given mass in a single cell).

3. Experiments.

3.1. Description of problems and processing of results. We study two special geometrical influences on two kinds of mesh topologies in 2D, for problems with uniform velocity field and Dirac-like initial condition for the advective transport.

The problems are chosen to make straightforward generalisation of 1D problem, or more precisely of a 2D problem where the velocity is parallel to the mesh sides (i.e. with zero numerical transport in the transversal direction just like in the 1D). The first case is random perturbation of the mesh point positions, causing the sides to be slightly non-parallel to the velocity and the mass transfer in transversal direction to appear. The second case is the "rotation" of the velocity direction with respect to the directions of the mesh sides, leading to a bit more complex anisotropic behaviour of the numerical mass transfer.

Besides that, we also observe the influence of the Courant number, which is the substantial measure of numerical diffusion in the 1D problems.

3.1.1. Computational meshes. We use the following two mesh topologies: one composed of equilateral triangles (denoted as "triangle" below) and the second composed of right triangles paired to squares (denoted as "square" below). A rhomboidal domain for the first (Fig. 3.1 left) and a rectangular domain for the second (Fig. 3.1 right) are considered.

The length of triangle edges is 10m (except of diagonals), meaning the equivalent step in 1D problem $\Delta x = 5$m. Considering the velocity $v = 1$m/d and time step $\Delta t = 5$d, we obtain the Courant number around 0.5 (changes slightly with mesh perturbation and velocity directions).

3.1.2. Model problem to solve. The solved transport problem is chosen so that the advection-dispersion equation with uniform velocity field and anisotropic

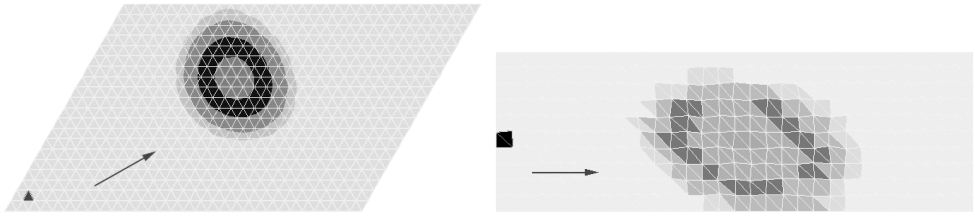

FIG. 3.2. *Visual expression of the numerical diffusion behaviour: the distribution of concentration in final time vs. the initial distribution (single black triangle/square), the arrows express the direction of water flow.*

dispersion (two coefficients) has an analytical solution: for the initial condition given by the Dirac δ-function in the point $[0,0]$, the solution is[1]

$$\tilde{c}(x,y,t) = \frac{M}{4\pi d\sqrt{D_L D_T}\, t} \exp\Big[- \frac{(x - v_x t)^2}{4D_L t} - \frac{y^2}{4D_T t}\Big] \tag{3.1}$$

where M/d is a dimensional factor (M corresponds to the total "injected" mass and d correspond to "thickness" of the 2D domain), the velocity is parallel to x axis (without loss of generality) with the component v_x, and D_L and D_T are the diffusion/dispersion coefficients in longitudinal and transversal directions respectively.

In the comparisons, the appropriate coordinate transformation (movement and rotation) is used, whereas independent rotation of velocity direction and rotation of principal directions of dispersion are considered. The angle of advective movement is determined by the given velocity (angle θ with respect to the original x axis), while the angle of dispersion direction (angle ϕ between the direction of higher dispersion and the original x axis) is a subject of identification in the experiments.

3.1.3. Method of comparison. We compare the results of the FV upwind model of advection with analytical solution of the corresponding advection-dispersion problem in all mesh points in the final time of computation ($t = 200$d). The measures of fit are the maximum absolute difference and the relative standard deviation

$$dev = \frac{1}{\max(\tilde{c}_i)} \sqrt{\sum_{i=1}^{N} \frac{(C_i - \tilde{c}_i)^2}{N-1}}\,, \tag{3.2}$$

where C_i are model results, $\tilde{c}_i$ are values of analytical solution, i is the cell index, and N is the number of cells.

The identification of numerical diffusion is done by minimizing the measures of difference by setting the values D_L and D_T and the angle ϕ of the characteristic directions of the dispersion (orientation of the isoline ellipses) with respect to x axis. Besides these measures, for initial estimates and for cases of non-uniqueness, an "optical" comparison of cross-section profiles was used (shape of gaussian curves).

3.2. Influence of mesh perturbation. In this case, the identification of numerical diffusion is quite clear: the numerical scheme produces a distribution of concentration in a shape of gaussian curve with different width in two orthogonal direction

[1] We remark that the computational domain is sufficiently large so that it can be replaced by the infinite domain concerning the solution of dispersion problem.

TABLE 3.1
Numerical diffusion on meshes with perturbation of node position. Dependence of coefficients on variance of perturbation, for the two types of mesh (triangles and squares).

variance (m)	D_L^{tri} (m^2/d)	D_T^{tri} (m^2/d)	D_L^{sqr} (m^2/d)	D_T^{sqr} (m^2/d)
0.1	1.25	0.04	1.25	0.055
0.2	1.3	0.06	1.3	0.075
0.5	1.3	0.2	1.3	0.18
1	1.95	0.5	2.05	0.5
2	2.35	0.9	2.8	1.5

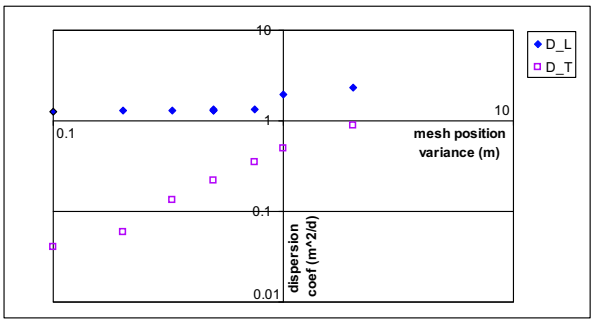

FIG. 3.3. *Longitudinal and transversal dispersion (m^2/d) in equilateral triangular mesh, in dependence on variance of random perturbation of mesh point positions (m).*

(Fig. 3.2 in the right). Typically, the numerical diffusion is stronger in the direction of velocity, except of cases with Courant number close to 1 (see the subsection 3.4).

Taking into account the 1D estimate of numerical diffusion, we can compare the results with the case of no perturbation, which is equivalent to 1D as the velocity is parallel to a certain set of cell sides. For the used parameters (v, Δx, Cr, section 3.1), we derive the 1D numerical diffusion coefficient $D_{\mathrm{num}} = 1.25$.

The results for both mesh topologies (triangular and rectangular) are given in Tab. 3.1, the triangular case also in Fig. 3.3. The possible values of perturbation variance are limited by technical aspects: If the perturbation is too small, the transversal transport influences just two neighbouring rows of cells, which is not representative enough for curve fitting. If the perturbation is too large, the topology of mesh points and their connections is lost.

We observe that for smaller variance (below 1m), the longitudinal coefficient D_L is almost constant and approximately equal to the value in 1D (i.e. unperturbed mesh). Together, the transversal coefficient D_T rises with rising variance, and the results for both type of meshes are similar. The continual change from the 1D-symmetry case is thus well confirmed. The results for higher values of variance show different trend and also differ between the mesh types.

3.3. Influence of mesh and velocity directions. Only the "triangle" mesh was used for this experiment, to exclude another source of anisotropy, caused by the orientation of the diagonals in the square mesh. Thanks to the symmetry of the mesh, the interval for angle between 0 and 30 degrees covers all the possible situations. The set of angle values 0, 3.3, 6.7, 10, 20, 30 (deg) is representative to demonstrate the behaviour.

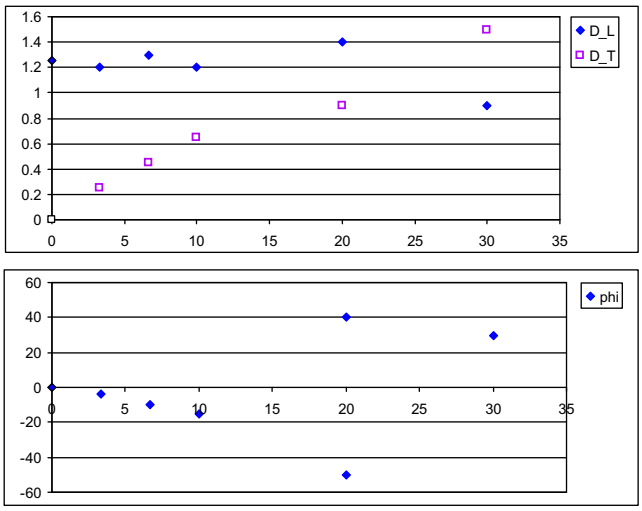

FIG. 3.4. *Dispersion coefficients (longitudinal and transversal) and angle of rotation of principal directions with respect to the mesh (equilateral triangles), in dependence on angle of velocity to the axis (m^2/d, deg).*

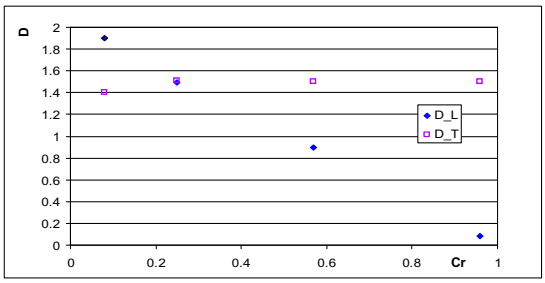

FIG. 3.5. *Influence of Courant number to the longitudinal and transversal dispersion for triangular mesh and* $\theta = 30$deg.

The zero angle corresponds to 1D-symmetry (as mentioned above) and $\theta = 30$deg is "left-right isotropic", i.e. no rotation of ellipses of concentration isolines with respect to the direction of velocity (see also Fig. 3.4 and Fig. 3.2 left). The behaviour for angles in between is quite complicated: the isoline ellipses rotate in opposite sense that the velocity with respect to the mesh, and with rising angle up to 30deg, the principal directions exchange (the direction longitudinal for $\theta = 0$ transform to transversal for $\theta = 30$deg). In fact except of the limit values of angles, the terms longitudinal and transversal lose their meaning.

3.4. Influence of Courant number. This analysis is understood as an extension of previous studies. We performed experiments for few special cases, which are representative for the overall trend.

In general, the Courant number determines the numerical diffusion process in the direction of velocity. For perturbed meshes, it simply means the longitudinal dispersion. For $\theta = 30$deg (Fig. 3.5), the situation is similar (as the behaviour is almost isotropic), while for $\theta = 6.7$deg, the anisotropy (rotation of isoline-ellipses with respect to the direction of velocity) is substantially influenced: very strong for

$\mathrm{Cr} \to 1$ while smaller for $\mathrm{Cr} \to 0$.

A typical behaviour for isotropic problems is the following: The transversal coefficient is almost constant (given e.g. by mesh perturbation or mesh structure itself) and the longitudinal coefficient given approximately by the relation (2.6) for 1D case.

4. Conclusion. We determined substantially different cases of behaviour of the numerical diffusion. For flow velocity parallel to mesh (perturbed) or for the left-right symmetric case, the numerical diffusion resembles the dispersion process in porous media in sense of two dispersion coefficients in the direction of velocity and the direction orthogonal to it. The diffusion/dispersion in the longitudinal direction is given by the Courant number according to the 1D relation (2.6) and in the transversal direction is given by structure of the mesh. Moreover, (2.6) gives a correspondence between the porous media dispersivity α_L [1, 8] and the mesh step Δx, concerning the linear dependence on velocity $D_L = \alpha_L v$. In this sense, we extends the results in [7].

For the non-symmetric cases of velocity direction vs. characteristic directions of the mesh, the behaviour of the numerical diffusion is complicated: it does not correspond to gaussian function with the principal direction parallel to velocity, but mostly the difference is only in certain rotation of the isoline ellipses.

Thus for the studied class of problems (representing the typical cases in groundwater modelling), we have a basic estimate whether the numerical diffusion in the transport model can damage the results qualitatively or not: In perturbed and symmetric (30 deg) cases, the numerical diffusion can be interpreted as the hydrodynamic dispersion. The usual ratio 1:10 of transversal and longitudinal dispersion [8] is valid for the perturbation with the variance between 0.2m and 0.5m, i.e. 2–5% of the mesh step, and for $\mathrm{Cr} > \frac{1}{2}$. The difference from the correct ration in other cases is in one order of magnitude. For all the cases, including those with incorrect anisotropy, the numerical diffusion in all directions is bounded by the 1D relation for $\mathrm{Cr} \to 1$, i.e. $\frac{1}{2}\Delta x v$. To obtain more accurate and general results, it will be necessary to use larger set of model problem configurations in the experiments and as well useful to study the problem theoretically.

Accuracy of identification. The relative standard deviation between the model (numerical diffusion) and the analytical solution ("real" dispersion) in all the experiments is between 1 and 3 percents. In fact, this measure is influenced by the large number of almost-zero values in both compared sets. Quality of fit is better expressed by ratio of maximum absolute deviation to maximum values. This is about 10% for experiments with perturbed meshes and up to 20% for non-parallel velocity and mesh (higher for small angles).

Further consequences to real-world problems. Underground problems are typical with the large dimension in horizontal direction and small in vertical direction. Together with the velocity field influenced by drawing/injecting wells, it leads to the situation when Cr is small in most of the cells (quite few cells with higher velocity "block" the stability condition with high Cr). Thus the worst behaviour (in the sense of anisotropy) of numerical diffusion is avoided.

REFERENCES

[1] J. Bear and V. Verruijt, *Modeling groundwater flow and pollution*, D. Reidel, Dordrecht, Holland, 1990.

[2] C. Hirsch, *Numerical Computation of Internal and External Flows, Volume 1 – Fundamentals of Numerical Discretization*, John Wiley & Sons Ltd., 1991.

[3] M. Hokr, J. Maryška, and J. Šembera, *Modelling of transport with non-equilibrium effects in dual-porosity media*, in Current Trends in Scientific Computing, Chen, Glowinski, and Li, eds., Amer. Math. Soc., 2003, pp. 175–182.

[4] J. Maryška, M. Rozložník, and M. Tůma, *Mixed-hybrid finite-element approximation of the potential fluid-flow problem*, J. Comput. Appl. Math., 63 (1995), pp. 383–392.

[5] K. W. Morton, *Numerical solution of convection-diffusion problems*, Chapman & Hall, London, 1996.

[6] M. T. Odman, *A quantitative analysis of numerical diffusion introduced by advection algorithms in air quality models*, Atmospheric Environment, 31 (1997), pp. 1933–1940.

[7] D. Syriopoulou and A. Koussis, *2-dimensional modeling of advection-dominated solute transport in groundwater by the matched artificial dispersivity method*, Water Resources Research, 27 (1991), pp. 865–872.

[8] C. Zheng and G. D. Bennett, *Applied contaminant transport modeling*, Van Nostrand Reinhold, New York, 1995.